

Analysis of Dumbbell Shaped Defected Ground Structure with Low-Pass Filter at X-Band for Radar Application

Mohd Kamil Mohd Zahari

Jabatan Kejuruteraan Elektrik, Politeknik Seberang Perai

E-mail: m_kamil@psp.edu.my

Mohd Azlishah Othman

Centre for Telecommunication Research and Innovation,

Fakulti Kej. Elektronik dan Kej. Komputer,

Universiti Teknikal Malaysia Melaka

E-mail: azlishah@utem.edu.my

Abstract

In this paper, an improved periodic defected ground structure (DGS) with low-pass filter at X-band is analyzed. The dumbbell shaped DGS which are etched at the ground plane is chosen for this analysis. Initially, a filter is designed and simulated using identical DGS, and equally sized. By varying empirically the sizes of the DGS, an improved frequency response was obtained. So as to validate the performances of the proposed changes in the filter, simulation process was implemented between the uniform periodic DGS and the improved non uniform periodic DGS circuit. The result indicates the latter has better performance in the stopband with good transition band and suppressing ripples. The dumbbell shaped DGS with low-pass filter designed at cutoff frequency of 10 GHz, which is suitable for X-band in general and radar applications in particular. The equivalent circuits for the proposed dumbbell shaped DGS with low-pass filter and its matching LC parameters are given. The improved and proposed DGS with low-pass filter provides a size of $18 \times 7 \text{ mm}^2$ was fabricated. The measurement results show agreeable consistency with the simulated results.

Keywords: Dumbbell, Defected ground structure, Low-pass filter

1. Introduction

Nowadays, the development of a wireless telecommunication system occurs rapidly and exponentially. Filter is one of the crucial components in many RF/microwave applications and this include in the radar application. Various types of RF/microwave filter circuit has been developed and reported. A RF/microwave filter is a two-port device that plays the important role of controlling the frequency response at certain point of cross section in an RF/microwave system, letting a band of frequencies pass through while rejecting frequencies in other bands (Pozar, 2015). In other words, it is used to remove the unwanted frequency bands. Good design of RF/microwave filter can improve and enhance the quality of overall wireless communication systems.

With the rapid growth of the wireless communication industry, the demand of high performance RF/microwave filters is increasing. In current research, the efficient performance, low cost and compact size of filter structures are stringent consideration of the filter design. In order to get the better filter performance, electromagnetic band gap (EBG) also known as photonic band gap (PBG) and defected ground structures (DGS) has been introduced. These structures are applied in the design of microwave filters and provide undesired frequency bands rejection and size reduction of bulky microwave circuits (Challal et. al, 2011). These structures also can be easily modelled using simple RLC circuits, especially for microstrip line structures.

At present, there have been several latest concepts applied to distributed RF/microwave circuits. The technique includes defected ground structure or DGS, where the ground plane metal of a microstrip, stripline or coplanar waveguide circuit is modified to improve and enhance performance (Breed, 2008). This technique simply means that a “defect” has been placed in ground plane which is normally considered to be an approximation of an infinite, perfectly-conducting current sink. Beside that, a ground plane at radio or microwave frequencies is far removed from the idealized behavior of perfect ground. The additional perturbations of DGS not render as defective even though is it alter the uniformity of the ground plane (Ortega et al., 2011).

This research presents an analysis of a compact X-band microstrip low pass filter using non uniform dumbbell DGS array which brings advantages the dismissal of stubs and high impedance open lines, which are characteristic features of conventional designs. The characteristics of frequency response can be modified and adjusted by varying the size of the DGS form. The miniature size, high harmonic suppressions and sharp cutoff frequency response characteristics of the non uniform DGS filters are a priority for the requirements of modern communication systems (Mohra, 2011).

2. Methodology

A dumbbell shaped (square head) slot DGS was the design choice for this research. The choice is related the simplicity of manufacture and adjustments of dimensions. Figure 1 shows a microstrip line with DGS and the result by EM-simulation. As an example based on previous research, a, b, w and g, which are the dimensions of the DGS section, have been chosen to be 2.4, 1.6, 1 and 0.3mm, respectively. The substrate for the simulations was an RT/Duroid 5880 with 0.127mm-thick and a dielectric constant ϵ_r of 2.2. There is an attenuation pole near 18.6GHz in the field simulation result. Figure 1 shows the one-pole low-pass filter with an attenuation pole. In order to clarify the cutoff and attenuation pole property of the proposed DGS section simultaneously, the equivalent circuit should show performances of low-pass and band-stop filter at the same time. Therefore, the equivalent LC circuit shown in Figure 2 can clarify the phenomenon for the proposed DGS section.

2.1 Analysis Of Dumbbell Shaped DGS LPF With Periodic Structure

By cascading DGS cells, the depth and bandwidth of the stopband of the filters are inclined to depend on the number of periods. Period DGSs care about parameters including the shape of unit DGS, distance between two DGS units and the number of DGSs used. The proposed DGS circuit, comprised of the five-etched cells, is shown in Figure 5. Initially the distance between DGSs was made $\lambda_g / 2$ and gradually adjusted to the value of $d = 2.7\text{mm}$.

The EM-simulation result are shown in Figure 6(a). It is possible see a bandwidths and stopband well defined, in conformity with the characteristics of a low-pass filter. As expected in structures with distributed parameters the frequency response is periodic. For the simulation result verify that the periodicity of DGS is not a critical parameter for the shape of frequency response, Figure 6(a).

2.2 Analysis Of Dumbbell Shaped DGS LPF With Different Dimensions

Figure 10 shows the effect of geometric dimensions of the DGS in response frequency were analyzed. In recent research, dumbbells were analyzed a square head slot DGS, and reported that the etched slot width below the conductor line and area of the square head are related to the effective capacitance and inductance of the microstrip line (Arya et al., 2010).

In order to examine the influence of the square slot head dimension, the etched slot width and the length were kept constant to 0.2mm and 1.7mm in all three cases and the square slot head was varied. The substrate with 1.6mm thick and a dielectric constant $\epsilon_r = 4.6$ was used for all simulations. Based on Figure 10, as the slot width is kept constant to 0.2mm, the capacitance values are same for all cases. The increase of the square head area's enlarges the effective series inductance, resulting in a lower cutoff frequency.

The attenuation poles in EM-simulation results are becoming almost to the low frequencies, as the square head area increase. These attenuation poles can be explained by the capacitance in parallel with the series inductance. The attenuation pole location, which corresponds to the resonance frequency of the parallel LC circuit, also becomes lower because as the series inductance increases, the resonance frequency of the equivalent parallel LC circuit decreases (Boutejdar et al., 2008).

3. Modeling And Parameter Extraction

The circuit parameters for the obtained equivalent circuit can be extracted from the EM-simulation result. The EM-simulation result of the proposed DGS unit section can be suited to the one-pole Butterworth-type low-pass response, which has 3dB cutoff frequency at 9.34, 10.30 and 12.01GHz. the series reactance value shown in Figure 2 can be calculated by using the prototype element value of the one-pole Butterworth response. The prototype element value is given by diverse references (Matthaei, 1980 & Arya et al., 2010). The parallel capacitance value for the given DGS unit dimension can be extracted from the resonance frequency, and prototype low-pass filter characteristics by using the subsequent procedures. The reactance value of the proposed DGS unit can be articulated as follows:

$$X_{LC} = (1/\omega_0 C) ((\omega_0/\omega) - (\omega/\omega_0)) \quad (1)$$

where:

ω_0 = resonance angular frequency of the parallel LC resonator, which is similar to attenuation pole location in Figure 10.

The series inductance of the Butterworth low-pass filter, as shown in Figure 11, can be articulated as follows:

$$X_L = \omega' \cdot Z_0 g_1 \quad (2)$$

where:

ω' = normalized angular frequency

Z_0 = scaled impedance level of the in/out terminated ports

g_1 = prototype value of the Butterworth-type low-pass filter pass filter

So as to have the low-pass filter characteristics, the equivalent circuit of proposed DGS unit section, as shown in Figure 2, must be equal to the prototype low-pass filter, as shown in Figure 11, at a particular frequency.

The prototype and its value of the Butterworth-type low-pass filter for the proposed DGS unit sections is as shown in Figure 12.

Where $g_0=1.0000$, $g_1=0.3473$, $g_2=1.0000$, $g_3=1.5321$, $g_4=1.8794$, $g_5=2.0000$, $g_6=1.8794$, $g_7=1.5321$, $g_8=1.0000$, $g_9=0.3473$ and $g_{10}=1.0000$.

The equivalence at the cutoff frequency of the low-pass filter is specified:

$$X_{LC|\omega=\omega_c} = X_{LC|\omega'=1} \quad (3)$$

Based on above equivalence, the series capacitance C of the equivalent circuit, as shown in Figure 2, can be calculated as follows:

$$C = (\omega_c/Z_0 g_1) \cdot (1/(\omega_0^2 - \omega_c^2)) \quad (4)$$

When the capacitance value of the equivalent circuit is extracted, the series equivalent inductance for the given DGS unit section can be obtained as follows:

$$L = 1/(4\pi^2 f_0^2 C) \quad (5)$$

where:

f_0 = resonant frequency

C = extricated series capacitance value

Table 1 shows the extracted equivalent circuit parameters for the proposed DGS unit sections.

4. Experimental Results

The optimized dumbbell shaped DGS LPF was fabricated on a substrate with a relative dielectric constant ϵ_r of 4.6 and a thickness h 1.6mm. A line width of 1.5mm was used, corresponding to 50Ω line for conventional microstrip line. The dimensions, the gap and the slot lengths are specified in Figure 13. The distance between each DGS is different, where $d_1 = 1.8\text{mm}$ and $d_2 = 1.5\text{mm}$. The photograph of the fabricated DGS and measurement result is shown in Figure 14 and Figure 15 respectively.

The measured performance compared with simulation result results are shown in Figure 16. The cutoff frequency measured at 10.35GHz and the stopband attenuation can be considered satisfactory with loss of more 10dB, between 10.0 and 12.0 GHz, ($\Delta f = 2\text{GHz}$). It is observed that the realized LPF has a frequency response shifted, when compared with the simulated LPF. One can see from Figure 16 is the measurement results show agreeable consistency with simulated ones.

5. Conclusion

This paper presents the design and analysis of dumbbell shaped DGS with low-pass filter at X-band for radar application. Periodic non uniform dumbbell shaped DGS with low-pass filter at X-band has been simulated, fabricated and measured. The properties of frequency response can be modified by changing the dimension size of the DGS structure. The fabricated DGS with low-pass filter shows the cutoff frequency at 10.35 GHz, 15.9 dB insertion loss with small ripples in the passband.

The compact size and modesty of the structure make the proposed DGS with low-pass filter a strong nominee for applications in various modern microwave circuits in general and radar in particular.

6. Acknowledgment

Authors would like to thanks Dr. Mohamad Zoinol Abidin Abd. Aziz for his invaluable guidance and advice. Last but not least, to all those who had directly and indirectly contributed towards the completion of this research.

References

Ahn, D., Park, J. S., Kim, C. S., Kim, J., Qian, Y., and Itoh, T., 2001. A Design of the Low-Pass Filter Using the Novel Microstrip Defected Ground Structure. *IEEE Transaction on Microwave Theory And Techniques*, vol. 49, no. 1, pp. 86-93

Arya, A. K., Kartikeyan, M. V., and Patnaik, A., 2010. On the Size Reduction of Microstrip antennas with DGS. In: *IRMMW-THz, International Conference on Infrared Milimeter and TeraHertz Waves*.

Boutejdar, A., Omar, A., Batmanov, A., Burte, E. P., and Elsherbini, A., 2008. A Simple Method to Control the Reject Band of Microstrip Low Pass Filter Using a New Multi-Ring Defected Ground Structures (DGS). In: *IEEE, Antennas and Propagation Society International Symposium 2008*, pp. 1-4.

Breed, G., 2008. An Introduction to Defected Ground Structures in Microstrip Circuits. *High Frequency Electronics*, Summit Technical Media, LLC, pp. 50-54.

Challal, M., Labu, F., Dehmas, M., and Azrar, A., 2011. Comparative Study of Three DGS Unit Shapes and Compact Microstrip Low-Pass and Band-Pass Filters Designs. *World Academy of Science, Eng. and Tech.*, vol 59, pp. 1582-1586.

Matthaei, G. L., 1980. *Microwave Filters, Impedance Matching Networks and Coupling Structures*. Norwood, MA: Artech House. pp. 217-228.

Mohra, A. S., 2011. Compact Lowpass Filter with sharp Transition Band based on defected Ground Structures. *Progress In Electromagnetics Research Letters*. vol. 8, pp. 811-815.

Ortega, A., Leonardo R. A. X. de Menezes, Martins Soares, A.J., and Abdalla Jr., H., 2011. Design of Low-Pass Microstrip Filters Based on Defected Ground Structure. In: IEEE, *Microwave & Optoelectronics Conference (IMOC)*, pp. 69-74.

Pozar, D. M., 2012. *Microwave Engineering*, 4th ed., New York: John-Wiley & Sons, pp. 380-450.

Appendices

Table 1. Extracted equivalent-circuit parameters for the proposed unit DGS section.

	DGS dimensions		
	(a x b) 1.2mm x 1.5mm	(a x b) 1.4mm x 1.8mm	(a x b) 1.6mm x 1.9mm
Inductance (nH)	0.0246	0.2157	0.2836
Capacitance (pF)	6.3612 $g_1= g_9$	0.9051 $g_3= g_7$	0.8535 g_5
Capacitance (pF)	2.2093 $g_2= g_8$	0.7379 $g_4= g_6$	
Cutoff frequency, f_c (GHz)	12.01	10.30	9.34
Attenuation pole location, f_o (GHz)	12.71	11.39	10.23

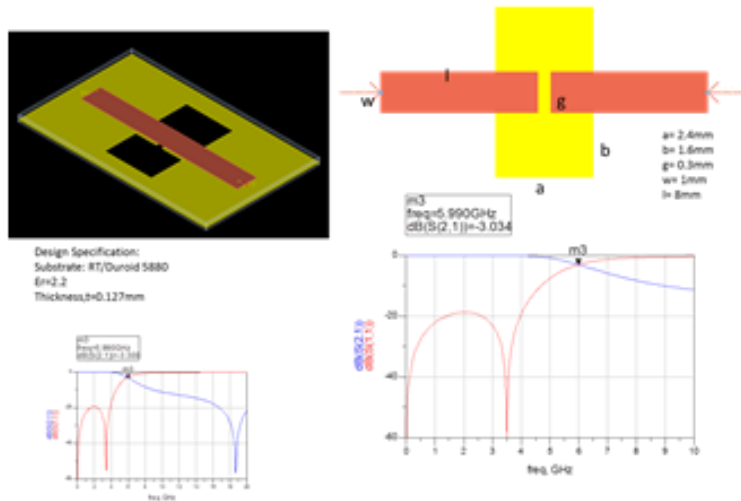


Figure 1. Simulated S-parameters of DGS unit section.

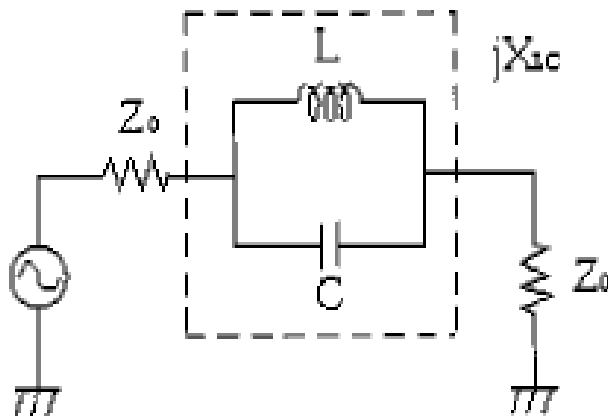


Figure 2. Equivalent LC circuit of the proposed DGS circuit. The dotted box indicates the DGS section.

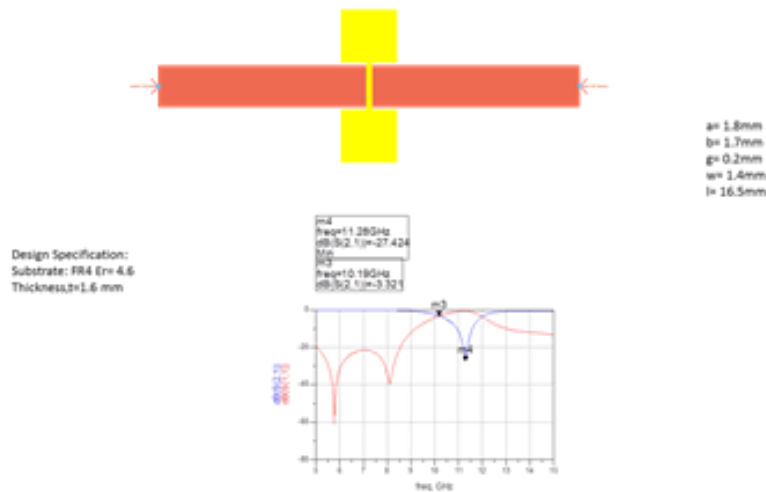


Figure 3. Simulated S-parameters of 1 dumbbell shaped DGS.

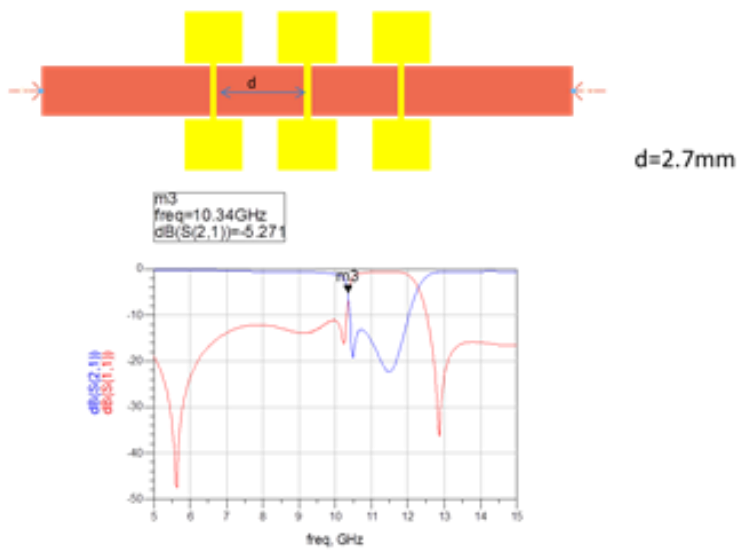


Figure 4. Simulated S-parameters of 3 identical dumbbell shaped DGS.

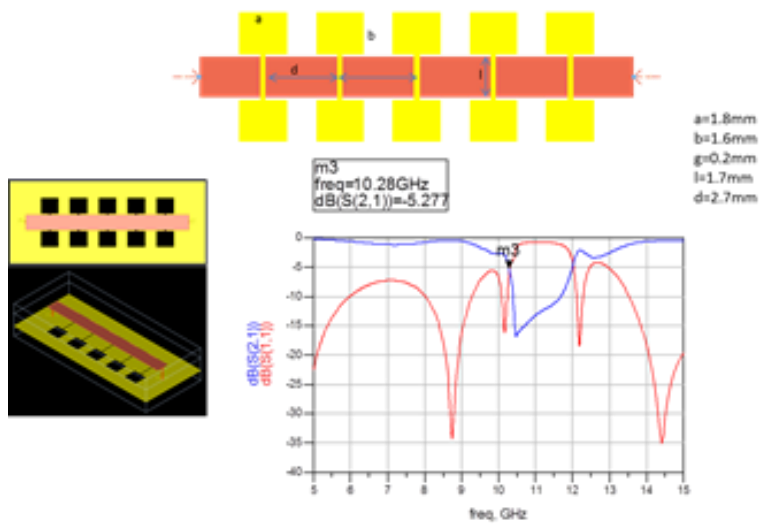


Figure 5. Simulated S-parameters of 5 identical dumbbell shaped DGS.

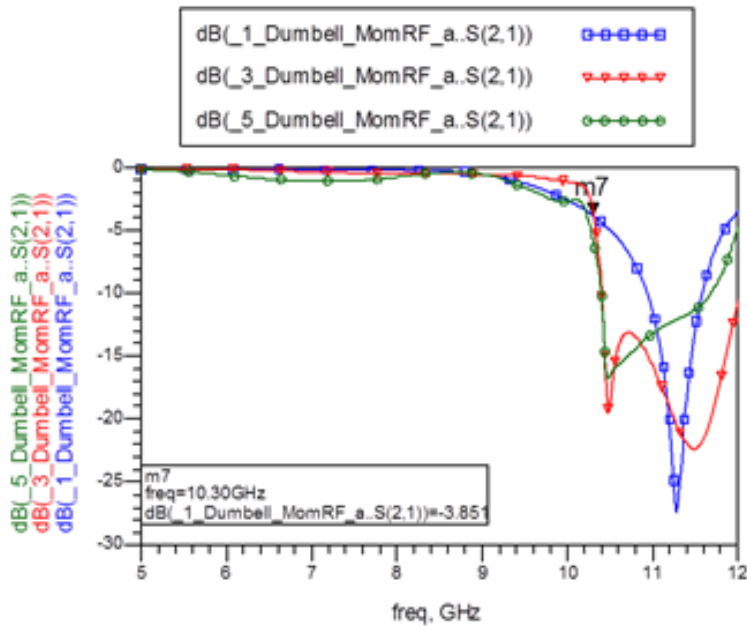


Figure 6(a). Comparison of simulation and measurement result - Insertion loss.

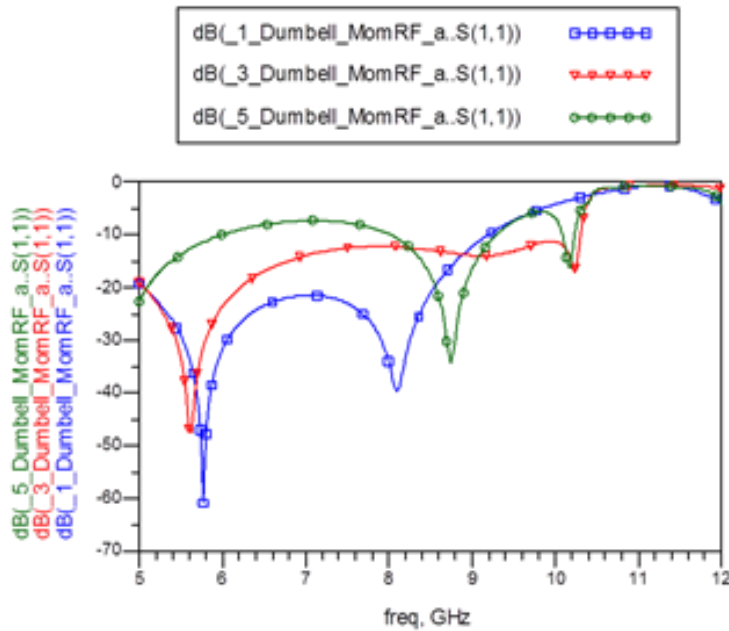


Figure 6(b). Comparison of simulation and measurement result - Return loss.

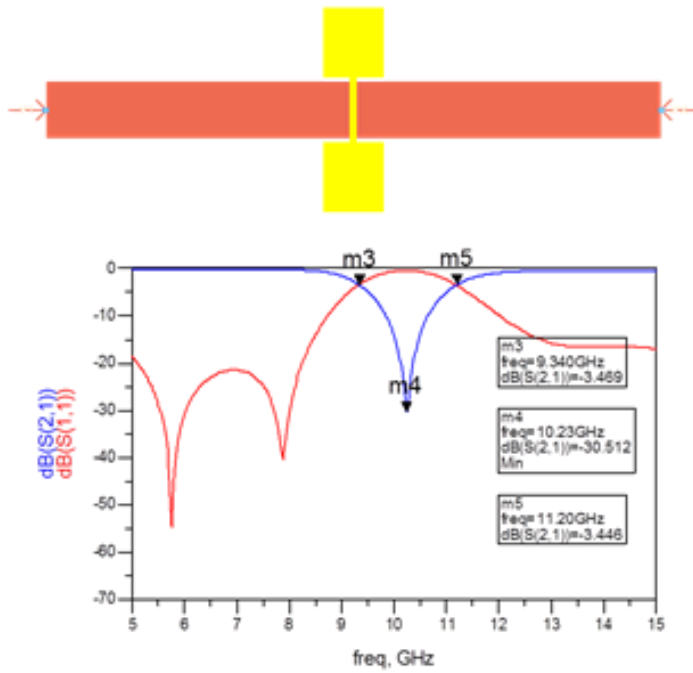


Figure 7. Simulated S21-parameter of 1st dimension. The dimensions a – 1.6mm and b – 1.9mm.

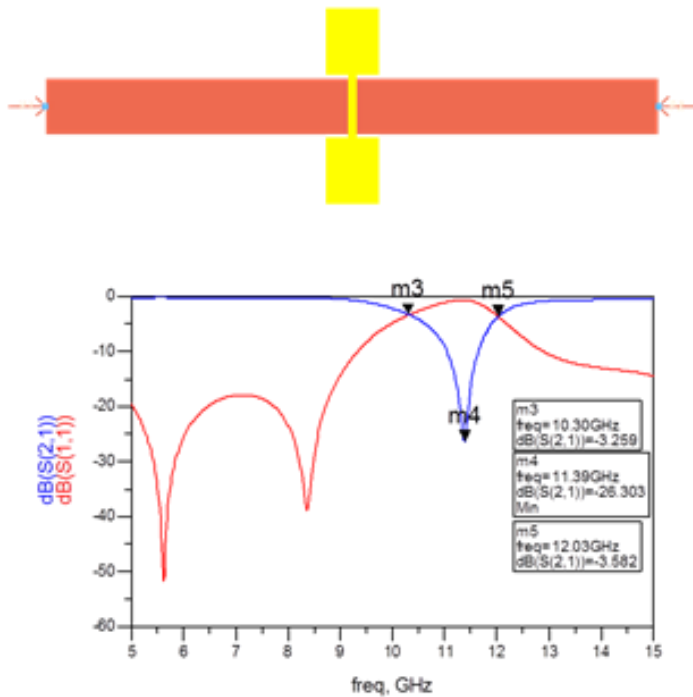


Figure 8. Simulated S21-parameter of 2nd dimension. The dimensions a – 1.4mm and b – 1.8mm.

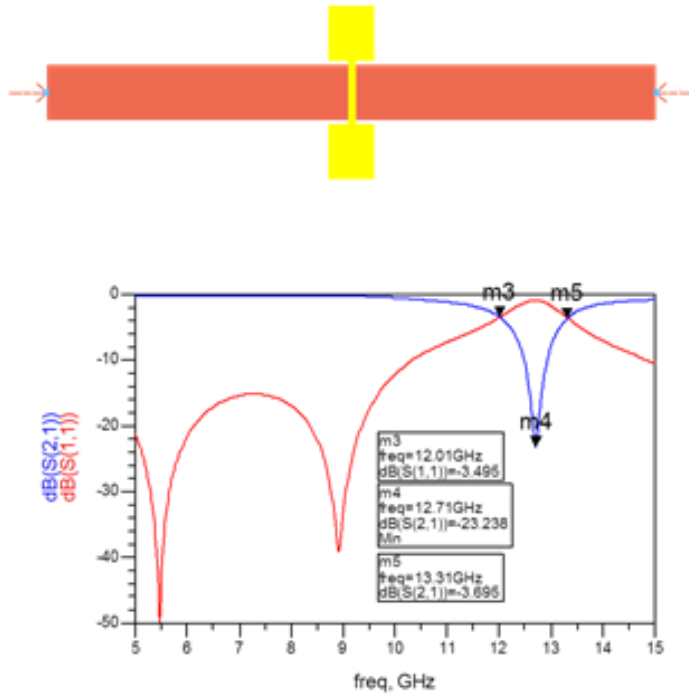


Figure 9. Simulated S21-parameter of 3rd dimension. The dimensions a – 1.2mm and b – 1.5mm.

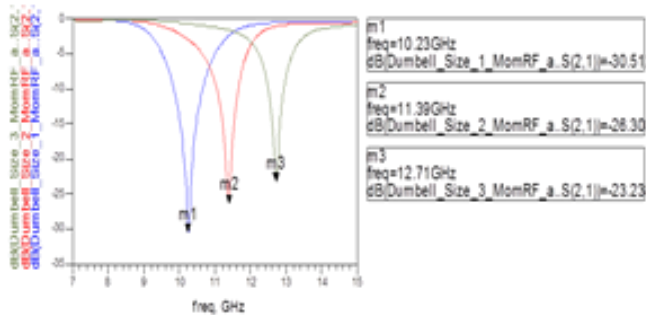


Figure 10. Comparison result of different dimensions 1st, 2nd and 3rd DGS - attenuation poles and cutoff frequency.

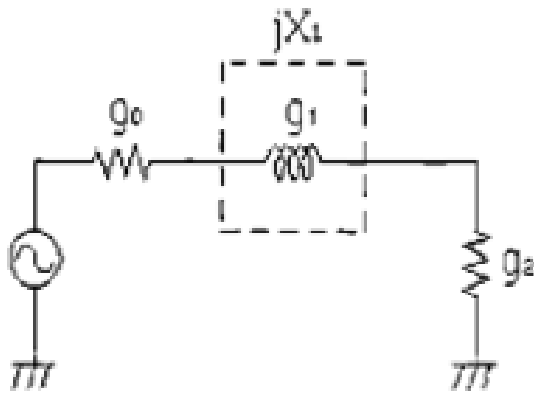


Figure 11. Butterworth-type prototype of one-pole LPF.

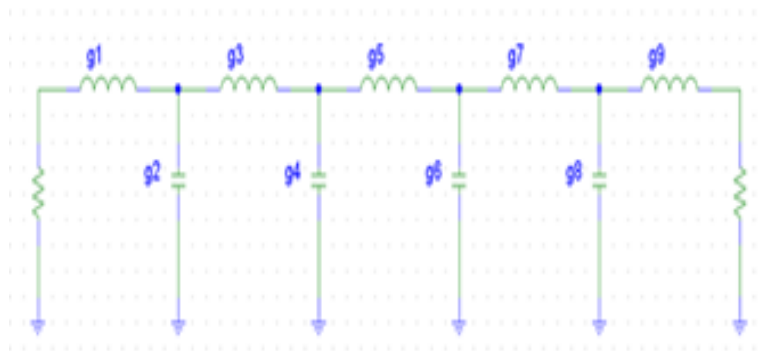


Figure 12. Butterworth-type prototype for the proposed DGS unit section.

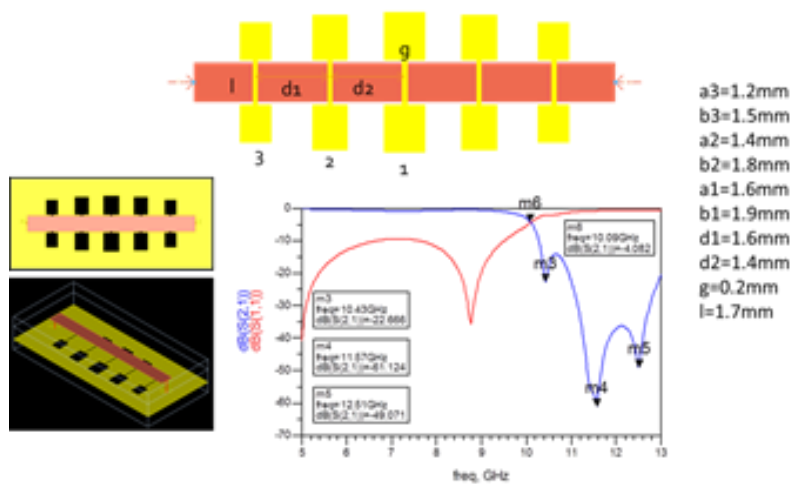


Figure 13. Simulation design and result – 5 non uniform periodic dumbbell shaped DGS LPF.

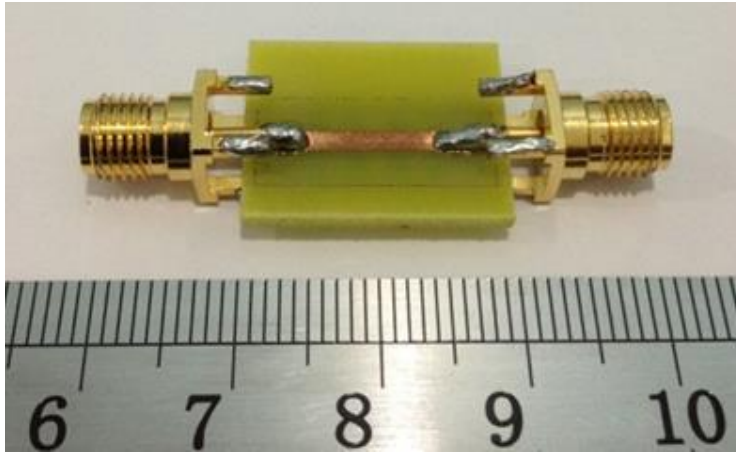


Figure 14(a). Fabricated dumbbell shaped DGS LPF – Top.

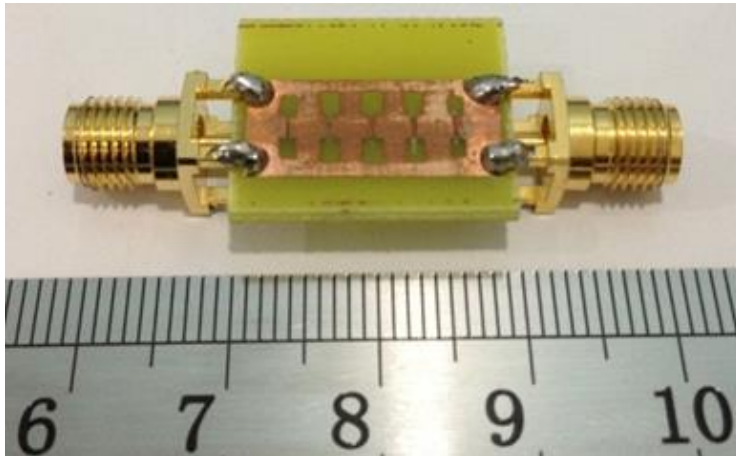


Figure 14(b). Fabricated dumbbell shaped DGS LPF – Bottom.

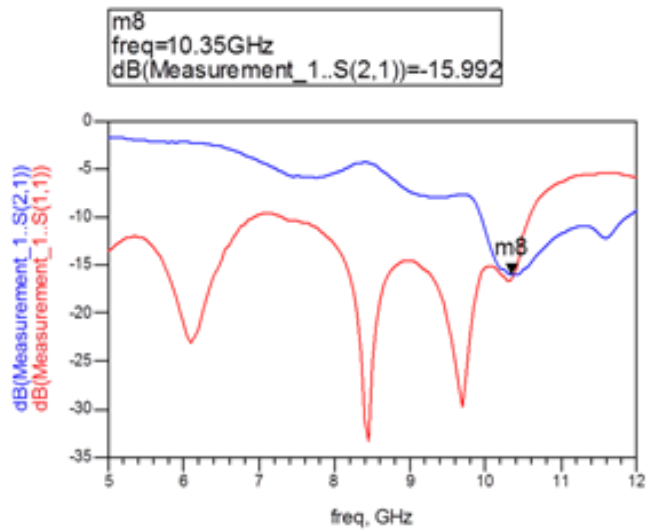


Figure 15. Measurement result – Insertion and return loss.

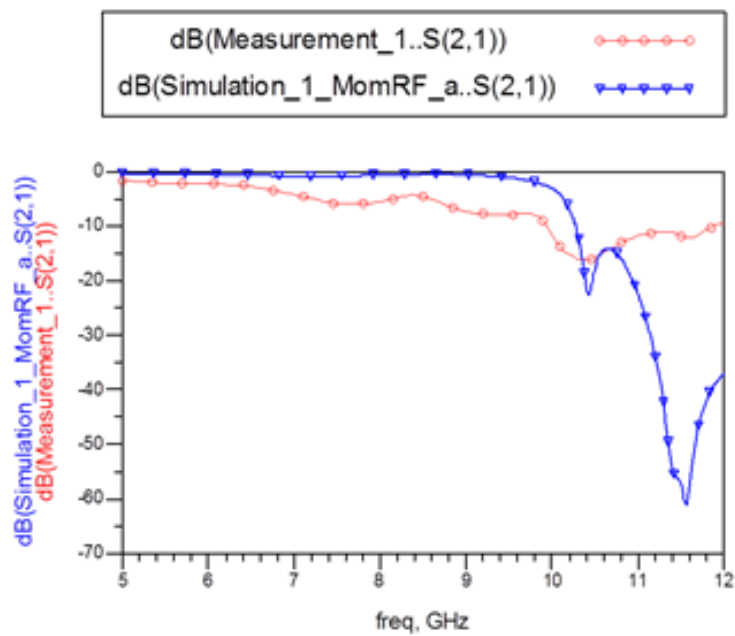


Figure 16(a). Comparison of simulation and measurement result - Insertion loss.

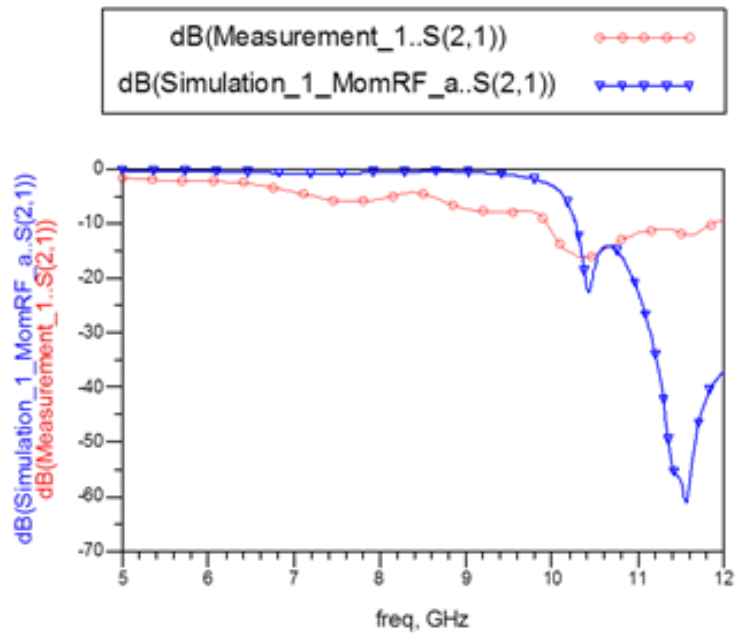


Figure 16(b). Comparison of simulation and measurement result - Return loss.